

Chapter 6

Performance of Geocell-Reinforced Sand Foundations with Clay Subgrades of Varying Strength



A. Murali Krishna , Arghadeep Biswas , S. B. Prasath, and Sujit Kumar Dash

Abstract This chapter provides an understanding of the performance of the geocell-reinforced sand foundations having clay subgrades of varying strengths. Model tests were conducted on a rigid circular model footing of 150 mm diameter (D) resting on foundation beds of different configurations prepared in a steel tank having dimensions of 1 m \times 1 m \times 1 m. Different foundation configurations were considered by varying thickness of reinforced and unreinforced sand layers overlying a wide range of subsoil strengths, from very soft to stiff clay, varying the undrained shear strengths (c_u) from 7 to 60 kPa. The results are presented in terms of bearing pressure and surface deformations responses at different loading stages. The results are further analyzed in terms of foundation reaction modulus, improvement factors, and percentage reduction in settlement. The outcomes of the study indicate that the geocell-induced improvement in the foundation performance is significantly influenced by the subgrade strength. For lower subgrade strength soil, the degree of improvement is highest, and it is decreased nonlinearly with increase in subgrade strength.

Keywords Clay subgrade \cdot Sand \cdot Geocell-reinforcement \cdot Bearing capacity improvement \cdot Settlement reduction

A. Murali Krishna (✉)

Department of Civil and Environmental Engineering, Indian Institute of Technology Tirupati, Tirupati, India

e-mail: amk@iittp.ac.in

A. Biswas

Department of Civil Engineering, Jalpaiguri Government Engineering College, Jalpaiguri, India

e-mail: arghadeep.biswas@gmail.com

S. B. Prasath

Department of Civil Engineering, Indian Institute of Technology Guwahati, Guwahati, India

e-mail: prasathcbt@gmail.com

S. K. Dash

Department of Civil Engineering, Indian Institute of Technology Kharagpur, Kharagpur, India

e-mail: sujit@civil.iitkgp.ac.in

6.1 Introduction

Soil reinforcement, in various forms, has been rigorously applied in several civil engineering applications, such as foundations, pavements, slopes, retaining walls, and embankments. In past few decades, soil-reinforcements are evolved through several modifications, in terms of material (metallic to geosynthetics) and type (two-dimensional planar strip, and sheet to three-dimensional geocell). Geocell is a three-dimensional honeycombing confining system of interconnected cells, made of thermally welded or mechanically bonded polypropylene and polyethylene materials. Readymade geocells are available commercially, which are easy to handle and transport in collapsed form and can be expanded as mattress at site (Fig. 6.1). They can also be made in field using planar geotextiles or geogrids as per required dimensions.

The benefits of planar reinforcements are demonstrated by Binquet and Lee (1975), Akinmusuru and Akinbolade (1981), Fragaszy and Lawton (1984), Khing et al. (1994), Mandal and Sah (1992), Sitharam and Sireesh (2004), and Biswas et al. (2015). As compared to planar form, geocell is a comparatively new invention in soil reinforcement, devised by Webster and Watkins (1977). Different studies have revealed its superiority over the planar reinforcements and/or various traditional ground improvement techniques, such as heavy compaction, soil replacement, and chemical stabilization. The advantage of using geocells is established through several applications, such as foundations, embankments, bridge abutments, gravity walls and steepened slopes, roadways, and railways. (Rajagopal et al. 1999).

Schematic configuration of a typical geocell-reinforced foundation system is shown in Fig. 6.2. To improve the bearing capacity of foundation soil, geocells are placed directly over the native soft ground, and then, the pockets of geocell are filled, preferably, with granular materials like sand which have better drainage properties and reinforcement interaction behavior. Two types of soils can be noticed in the figure: The Soil Type-2 is the native soil underneath the reinforced-soil, and the Soil Type-1 is geocell-reinforced/unreinforced fill soil. D is the diameter of the footing. H is the thickness of geocell-reinforced sand layer overlying the clay subgrade, d is the geocell opening size, u is the depth of placement of geocell-mattress below the

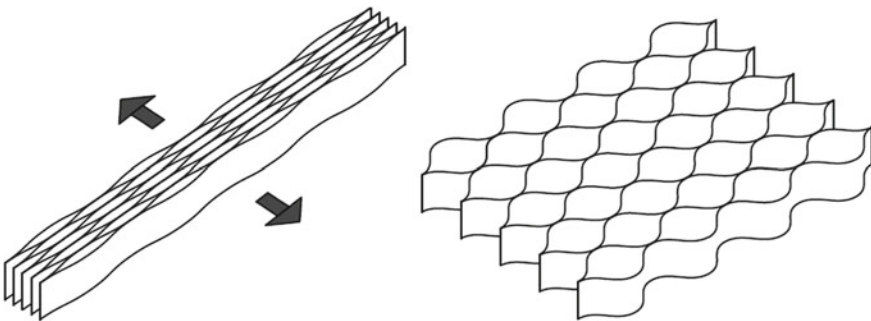


Fig. 6.1 Typical geometry of geocell (Yang et al. 2010)

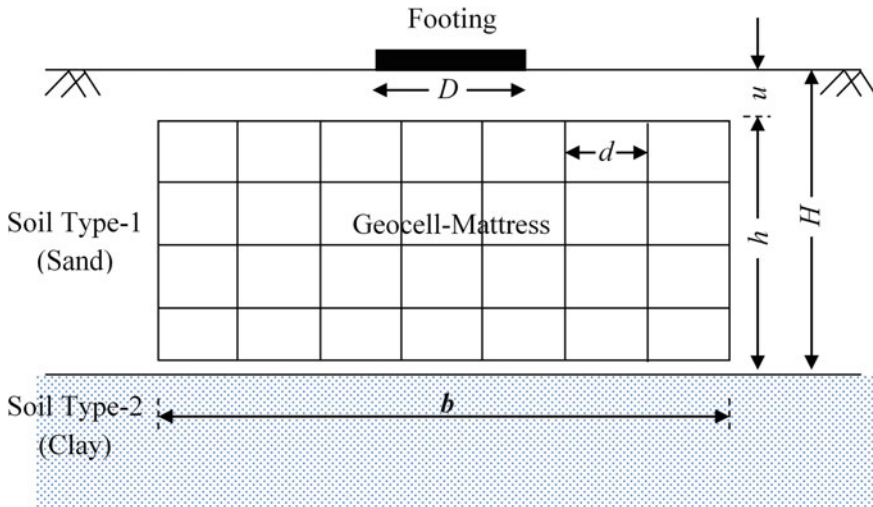


Fig. 6.2 Schematic configuration of geocell-reinforced foundation systems (after Biswas et al. 2016)

base of footing, b is the width of geocell-mattress, and h is the height of geocell-mattress. In practice, natural ground (subgrade) may exist at different strength levels, and situations may arise where reasonably strong soils also fail to meet the design requirements which need to be improved. In such situations, performance of reinforced foundations with different subgrade strengths should be considered. As can be seen in Fig. 6.1, the entire geocell-mattress is supported by the underlying subgrade. Hence, the behavior of geocell-reinforced foundation system is largely dependent on the underlying subgrade.

In view of this, the main objective of this chapter is to provide insight into the performance of geocell-reinforced sand beds resting on clay subgrades of various strengths. Biswas et al. (2013, 2015, 2016), Biswas (2016), performed various physical model tests with soil subgrades of varied strengths, from very soft to stiff clay, varying the undrained shear strengths (c_u) from 7 to 60 kPa overlain by geocell-reinforced sand mattresses of different heights. This chapter briefly describes the physical model tests conducted and presents the outcomes of model studies in terms of foundation reaction modulus, improvement factor, and percentage reduction in settlement.

6.2 Physical Model Tests

Model tests were carried out on a circular footing of 150 mm diameter (D) resting on 1 m \times 1 m \times 1 m foundation bed (test bed-cum loading frame assembly in the laboratory) having clay subgrades of different undrained shear strengths (c_u), ranging

Table 6.1 Material properties (Biswas 2016)

Material	Property	Value	
Clay (<i>CL</i>)	Specific gravity	2.65	
	Liquid limit (%)	42	
	Plastic limit (%)	21	
Sand (<i>SP</i>)	Specific gravity	2.68	
	Coefficient of uniformity	3.06	
	Coefficient of curvature	0.62	
	γ_d (kN/m ³)	Maximum	16.4
		Minimum	13.8
	Friction angle (ϕ°)	Direct shear	43
Triaxial compression		40	
Geocell (made of geogrid)	Geogrid aperture size (mm)	38 × 38	
	Tensile strength (kN/m) (at failure strain, %)	Geogrid	20 (at 11%)
		Bodkin joint	3.3 (at 9%)

from 7 to 60 kPa. Different series of laboratory model tests were performed on homogeneous and layered foundation systems. The layered systems were comprised of unreinforced and reinforced sand of varying layer thicknesses ($H = 0.63D$ to $2.19D$) overlying the clay subgrades. Two types of soils were used: a locally available clay soil for the subgrades and a river sand for the overlying layer. The geocell-reinforcements were formed using a biaxial geogrid through bodkin joints (with plastic dowel strips). A brief summary of the materials used and their properties are presented in Table 6.1.

6.2.1 Preparation of Clay Bed/Subgrade

A calibration curve (Fig. 6.3a) depicting the variation of shear strength with water content of clay, for a uniform compaction effort, was developed through a series of trial tests (details were presented in Biswas et al. 2015). The clay soil was pulverized, air dried, and mixed with the required water (as per the calibration curve) to achieve the desired shear strength. The wet soil was kept in sealed containers for about a week to get moisture equilibrium. The prepared clay was placed in the test tank and compacted in layers of 50 mm thickness, until the desired height was reached. In order to verify the uniformity, clay samples from different locations and layers were collected by pressing mold into the clay beds. The shear strength values of the samples were determined through vane shear apparatus and found to be with $\pm 2\%$ variation from the targeted shear strength values.

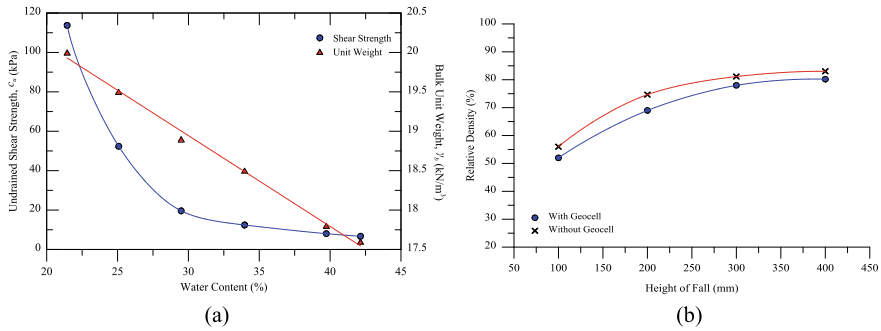


Fig. 6.3 Calibration curves: **a** for clay and **b** for sand (after Biswas 2016)

6.2.2 Preparation of Sand Bed

Sand beds were prepared through raining technique. The raining device consisted of a large container and a long hollow pipe having a 60° inverted cone connected at its bottom. By trial, the height of fall was adjusted to attain the required density in both reinforced and unreinforced cases, as shown in Fig. 6.3b. It may be noticed that to attain a desired density, the raining heights for geocell-beds were more compared to unreinforced case as higher energy was required to compensate the geocell-wall-interruption. Relative density (D_r) of sand was maintained as 80% ($\gamma_d = 15.83 \text{ kN/m}^3$) throughout the experimental program.

6.2.3 Geocell

The geocell-mattresses were prepared with geogrid strips, cut from a full roll into required dimensions, and assembled in chevron pattern using ‘bodkin’ joints (Simac 1990; Carroll and Curtis 1990; Biswas et al. 2015). The HDPE geogrid, with $38 \times 38 \text{ mm}$ aperture size, was having tensile strength of 20 kN/m at 11% of axial strain. The bodkin-dowels were 3 mm thick and 6 mm wide plastic strips, made of low-density polypropylene. Maximum tensile strength of the bodkin joints used was found to be 3.3 kN/m at axial strain of 9%. To prepare the geocell-mattress, the transverse and longitudinal geogrid members were cut from a long roll and assembled in ‘chevron’ pattern using ‘bodkin’ joints (Fig. 6.4).

6.2.4 Test Setup

The test setup for the experimental program is shown in Fig. 6.5. Foundation beds were prepared in a steel tank of $1 \text{ m} \times 1 \text{ m} \times 1 \text{ m}$ in dimension. The tank walls were

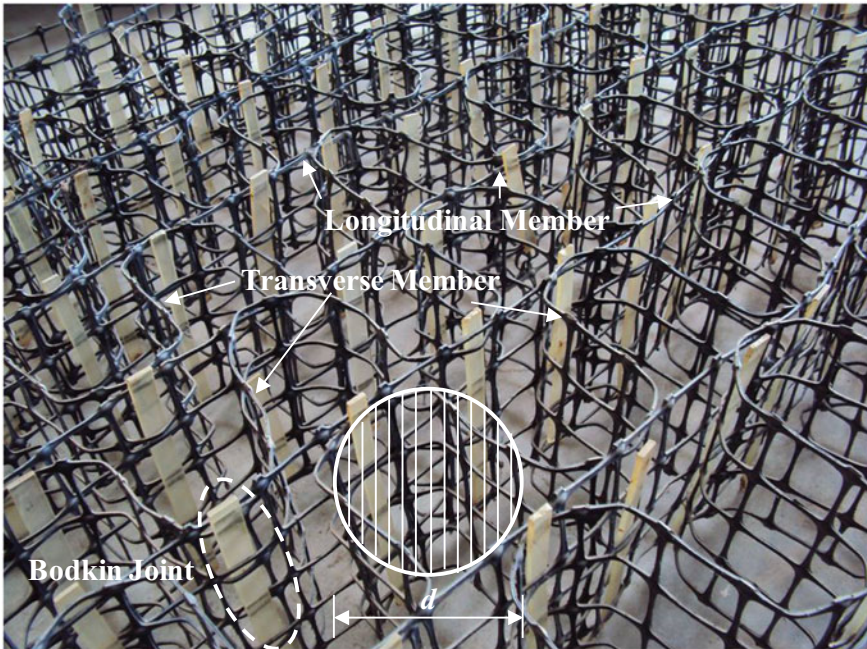


Fig. 6.4 Photograph of typical geocell-mattress in chevron pattern

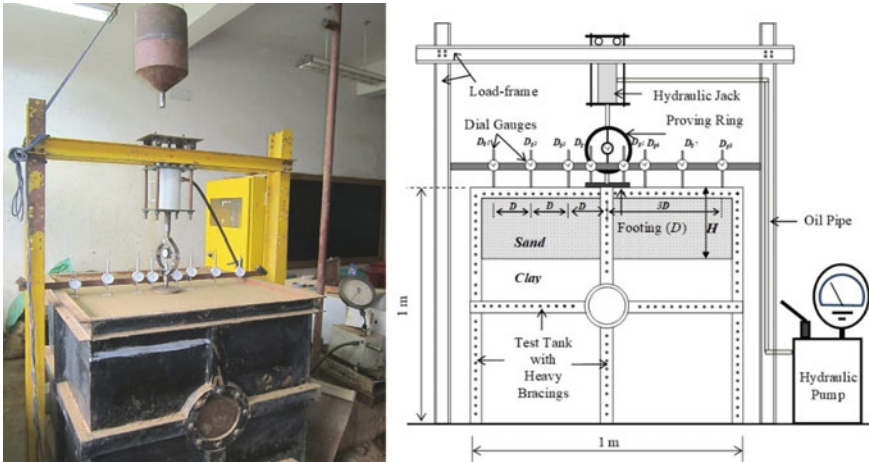


Fig. 6.5 Experimental setup (after Biswas et al. 2013)

well braced with heavy steel-sections (horizontally and vertically) to avoid lateral deformation, if any during testing. The test tank was provided with a loading frame for load application. The load was applied, by pushing the footing into the soil (at approximately 3 mm/min), through a hydraulic jack. The load applied was measured through a pre-calibrated proving ring, placed between hydraulic jack and footing. In order to ensure verticality of loading, a ball-bearing was positioned between proving ring and the footing. Responses of the model foundations were monitored at different loading stages by recording the deformations (heave or settlement) at different locations on the foundation surface through eight dial gauges (D_{g1} to D_{g8} shown in Fig. 6.5) of 0.01 mm accuracy. Two dial gauges (D_{g4} and D_{g5}) were placed diagonally opposite on the footing, while the other six were placed on the soil surface, at distances of D , $2D$, and $3D$. The spindles of these dial gauges were rested over small plates of perspex sheet placed on the foundation surfaces. Observations were recorded at regular intervals of footing settlement (s) and continued till the failure of foundation or up to $s/D = 24\%$.

6.2.5 Experimental Program

Tests were conducted on different homogeneous and layered configurations (unreinforced and reinforced) of foundations having varying clay subgrades under circular footing, as listed in Table 6.2. Pressure-settlement behavior of homogeneous sand and clay of varying strength was studied in series A. Unreinforced layered foundations with different thickness of sand layer ($H/D = 0.63, 1.15, 1.67$ and 2.19) over the clay subgrades of varying strength ($c_u = 7, 15, 30$ and 60 kPa) were studied in series B. The response of geocell-reinforced foundations with different subgrades was examined in series C. In total, 37 model tests were performed under three different test series (Table 6.2). In the layered configurations, the subgrade strength (c_u) and layer thicknesses (H) were varied keeping other parameters constant at their optimum (Biswas and Krishna 2017a).

Table 6.2 Details of model tests

Test series	Foundation system	Test parameters	
		Constant	Variable
A	Homogeneous clay and sand bed	–	c_u : 7, 15, 30, 60 kPa (clay) D_r : 80% (sand)
B	Unreinforced sand over clay subgrade	D_r : 80%	c_u : 7, 15, 30, 60 kPa H/D : 0.63, 1.15, 1.67, 2.19
C	Geocell-reinforced sand over clay subgrade	d/D : 0.8 u/D : 0.1 b/D : 6.67	c_u : 7, 15, 30, 60 kPa H/D : 0.63, 1.15, 1.67, 2.19 (h/D : 0.53, 1.05, 1.57, 2.09)

6.3 Test Results

The results obtained are presented as bearing pressure-settlement responses and footing settlement vs surface deformation graphs. Parameters such as sand layer thickness (H), height (h), and width (b) of geocell-mattress, depth of sand cushion on top of geocell-mattress (u), and footing settlement (s) are normalized with respect to the footing diameter (D) and expressed as H/D , h/D , b/D , u/D , and s/D , respectively.

6.3.1 Bearing Pressure—Settlement Behavior

A typical comparison of pressure-settlement responses of unreinforced and geocell-reinforced foundation systems, for $c_u = 7$ kPa, is presented in Fig. 6.6. Higher bearing pressures at larger footing settlements can be noticed. The geocell-reinforced bearing pressure is increased from 77 to 119 kPa, for the footing settlement (s/D) variation from 12 to 24% (at $H = 0.63D$). In similar foundation configurations, the variation of bearing pressures for unreinforced foundations was from 45 to 56 kPa. This indicates considerably high improvement in pressure values, for geocell-reinforced foundation systems as compared to unreinforced cases. Besides, it is seen that this improvement was increased with increasing settlement levels.

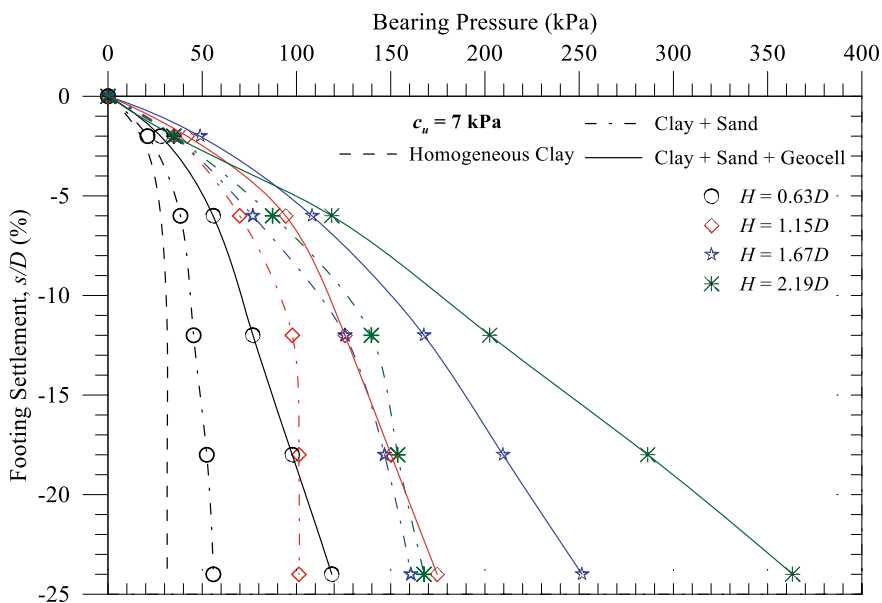


Fig. 6.6 Typical pressure-settlement responses for unreinforced and geocell-reinforced foundations (different H/D) with $c_u = 7$ kPa

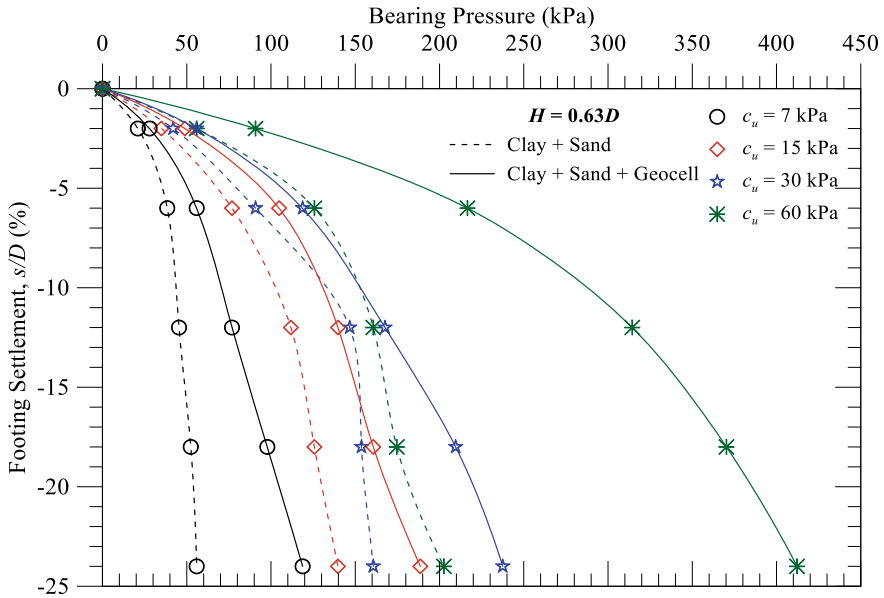


Fig. 6.7 Typical pressure-settlement responses for different clay subgrades with unreinforced and reinforced sand layer foundations with $H = 0.63D$ (after Biswas 2016)

The pressure-settlement responses showing the influence of subgrade strength on the performance of geocell-reinforced foundations (at $H = 0.63D$) are presented in Fig. 6.7. Substantial improvements, with higher bearing pressures for stiffer subgrades, can be noticed in the figure. The bearing pressures at $s/D = 24\%$ are 56, 140, 161, and 203 kPa for unreinforced layered systems having $c_u = 7, 15, 30,$ and 60 kPa, while bearing pressures were increased to about 119, 189, 238, and 413 kPa, respectively, with geocell-reinforcement.

6.3.2 Surface Deformation—Settlement Behavior

A typical surface deformation profiles of homogeneous bed ($c_u = 15$ kPa) at different levels of footing settlements (s/D) are presented in Fig. 6.8. The distance from the footing center ‘ x ’ is expressed in non-dimensional form as x/D . The surface settlement and heave are differentiated with ‘ $-$ ’ and ‘ $+$ ’ signs, respectively. It can be noticed that the surface deformations were mostly pronounced around the footing center (at $x = D$); while it was reduced as the distances increased (at $x = 2D$ and $3D$).

A typical variation of surface deformation (δ/D) with footing settlement (s/D) is shown in Fig. 6.9, for different foundation systems overlying clay subgrade of 7 kPa (c_u) at $H = 0.63D$. It can be noticed that as compared to the unreinforced foundations, the geocell-reinforced system has shown higher settlement at $x = D$

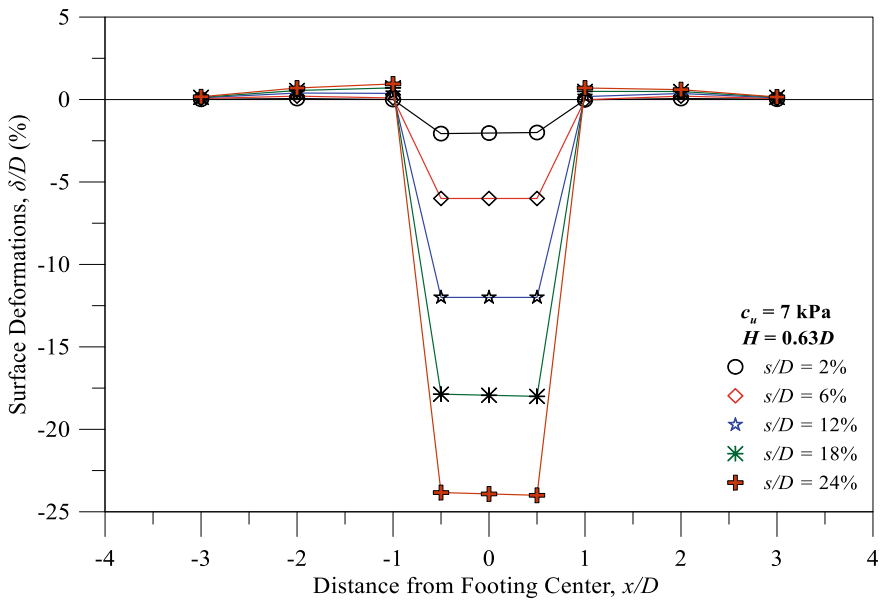


Fig. 6.8 Surface deformation profile at different s/D for $c_u = 15$ kPa

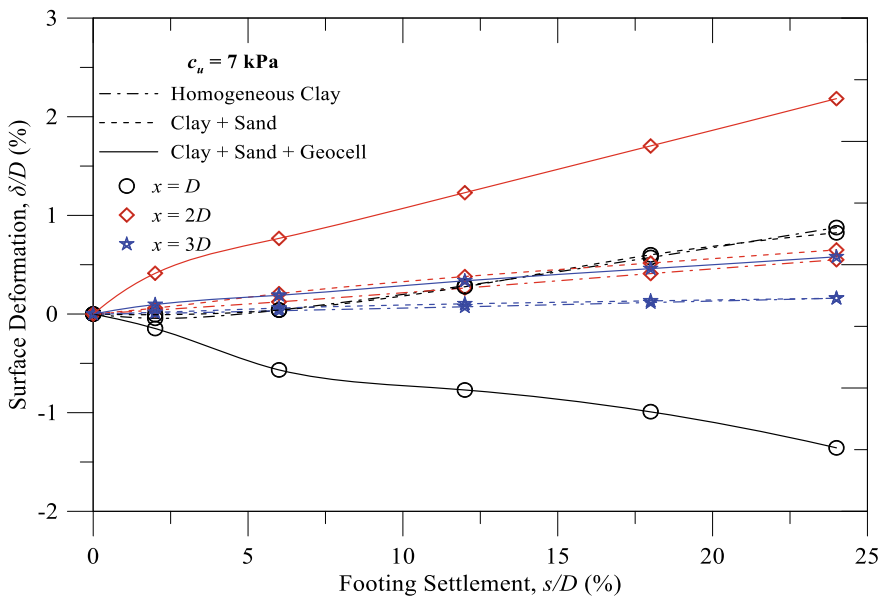


Fig. 6.9 Variation of δ/D with s/D at $x = D, 2D,$ and $3D$ for $c_u = 7$ kPa ($H = 0.63D$)

and more heaving at $x = 2D$ and $3D$. Such deformation profile is attributed to the deep beam action of geocell-mattress (Dash et al. 2003) which undergone sagging (causing settlement) around the footing center and hogging (causing heaving) away from the loading. However, the magnitude of deformations is dependent on thickness of geocell-mattress (h) and the strengths of the underlying subgrades (c_u).

Biswas et al. (2016) concluded that the sand layer thickness, $H = 1.15D$ has better performance among the performed four different sand layer thickness of $H/D = 0.63, 1.15, 1.67, \text{ and } 2.19$. The geocell-reinforced layered foundation has higher bearing capacity with reduced settlement compared to the unreinforced layered foundation. The beneficial effect was attributed to reinforcing action namely pocket all round confinement provided by geocell due to its cellular structure (Dash et al. 2003) and the interface frictional resistance from adjacent cells (Pokharel et al. 2010; Biswas et al. 2016). Besides, stiffness of geocell plays vital role in providing the degree of improvement of reinforced layer (Bathurst and Rajagopal 1993).

6.4 Interpretations of the Test Results

The test results obtained are analyzed and discussed in terms of the interpreted values, as foundation reaction modulus, improvement factor, and percentage reduction in settlement values for different foundation configurations.

6.4.1 Foundation Reaction Modulus, k_f

The foundation reaction modulus (k_f) is the secant modulus of the foundation system corresponding to a given settlement (slope of the line joining the origin to any point on pressure-settlement curve at the given settlement level). k_f values for model foundations with different configurations at different settlement levels were evaluated and presented herein.

Figure 6.10 presents the variation of k_f values with footing settlement (s/D) for different subgrades (c_u) and different foundation configurations (for $H = 1.15D$). In general, the figure indicates that k_f values decrease nonlinearly with increase in settlement levels for unreinforced foundations. A steep decrease of k_f in between 2 and 6% of s/D is followed by gradual reduction till the maximum level of settlements ($s/D = 24\%$). This behavior can be related to the surface deformation behavior of the foundation system. Biswas and Krishna (2017b) reported negligible surface deformation at initial settlement levels ($s/D < 6\%$) and from thereon the surface deformations increased with footing load till the end of test. However, in the case of reinforced foundations, the introduction of geocell-reinforcement enhanced the reaction modulus values significantly in comparison with the corresponding values for unreinforced (homogeneous and layered) foundations as shown in Fig. 6.10. For geocell-reinforced systems, the reduction in k_f with s/D is fairly linear. In this case,

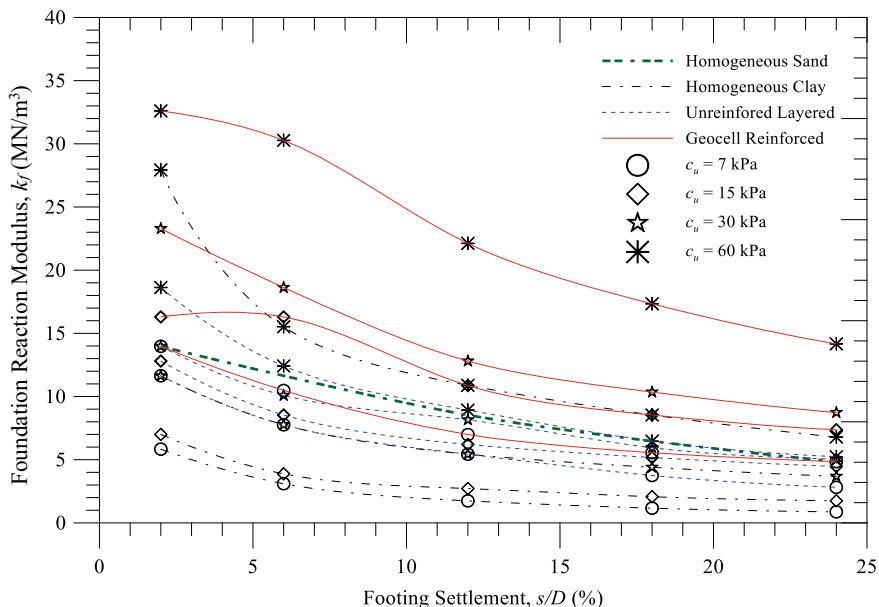


Fig. 6.10 Variation of k_f values with footing settlement (s/D) for different subgrades (c_u) and foundation configurations (with $H = 1.15D$)

geocell-pockets completely arrest the shearing of sand from footing bottom and cut the potential failure planes to force it deeper into the foundation beds making the geocell-sand bed as an elastic coherent layer. Besides, as reported by Biswas et al. (2013), the deformations at foundation surfaces also satisfy the confinement effect indicating significant reduction in surface heaving. Figure 6.11 shows the variation of k_f values with subgrade strengths (c_u) for different foundation configurations at different settlement levels ($s/D = 2, 6$ and 12%). It is to be noticed that the foundation reaction modulus increases for subgrade strength for any settlement level (s/D). In general, higher k_f values are found for superior foundation configurations, i.e., geocell-reinforced > unreinforced layered > homogeneous clay.

6.4.2 Improvement Factor, I_f

The ratio of bearing pressure of layered foundation to that of homogeneous clay bed foundation, at similar level of footing settlement, is defined as improvement factor (I_f). Three improvement factors, I_{fs} (Eq. 6.1), I_{fsgc} (Eq. 6.2), and I_{fgs} (Eq. 6.3), to represent the improvement of the geocell-reinforced foundation with respect to homogeneous clay and unreinforced layered foundation, are evaluated (refer Fig. 6.12) for different foundations at different settlement levels. The improvement factors evaluated for different foundation configurations are summarized in Table 6.3.

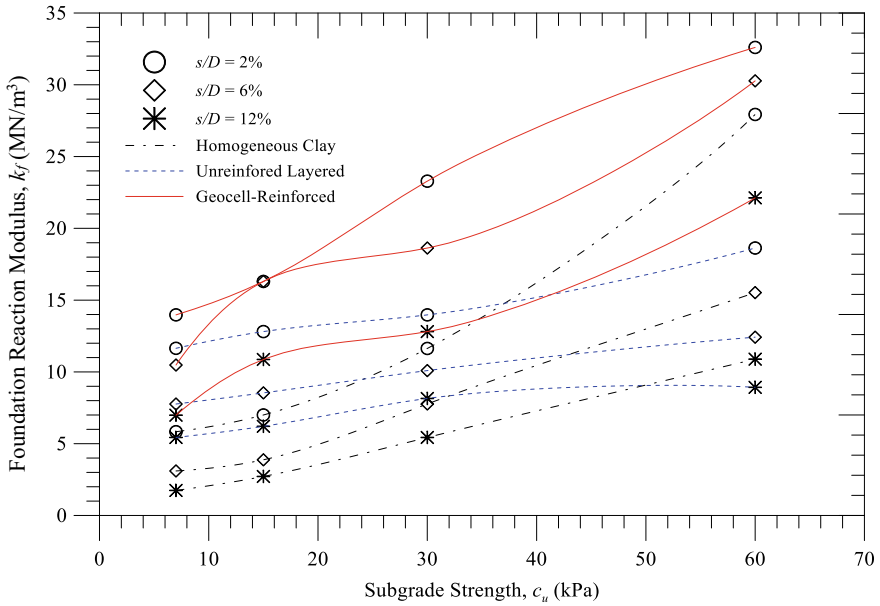


Fig. 6.11 Variation of k_f values with subgrade strength at $s/D = 2, 6$ and 12% for different foundation configurations (with $H = 1.15D$)

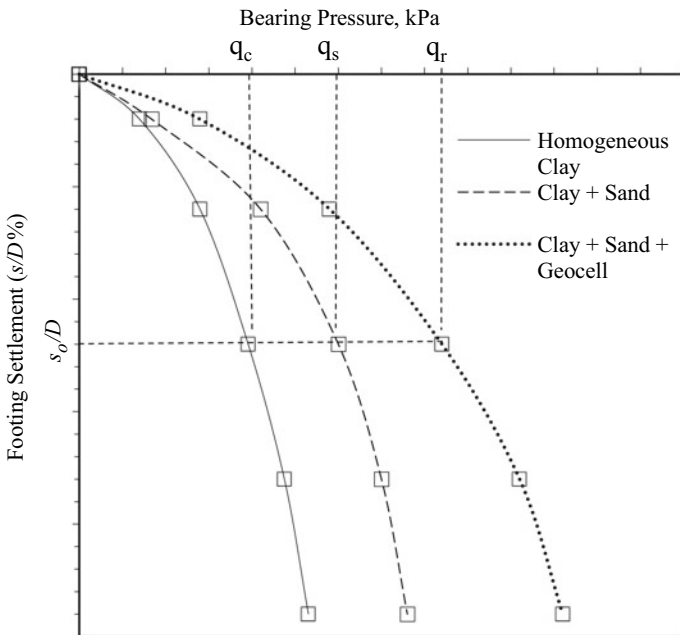


Fig. 6.12 Definition sketch of calculation of improvement factors

Table 6.3 Summary of bearing pressure improvement factors

s/D (%)	H/D	Bearing pressure improvement factor							
		$c_u = 7$ kPa		$c_u = 15$ kPa		$c_u = 30$ kPa		$c_u = 60$ kPa	
		I_{fsgc}	I_{fgc}	I_{fsgc}	I_{fgc}	I_{fsgc}	I_{fgc}	I_{fsgc}	I_{fgc}
2	0.63	1.60	1.33	2.33	1.40	1.60	1.33	1.08	1.63
	1.15	2.40	1.20	2.33	1.27	2.00	1.67	1.17	1.75
	1.17	2.79	1.40	2.66	1.45	2.20	1.22	1.00	1.71
	2.19	2.00	1.00	2.33	1.75	1.40	1.00	1.00	1.71
6	0.63	2.00	1.45	3.00	1.36	1.70	1.31	1.55	1.72
	1.15	3.38	1.35	4.20	1.91	2.40	1.85	1.95	2.44
	1.17	3.88	1.41	4.00	1.54	2.20	1.00	1.10	1.38
	2.19	4.26	1.36	3.60	1.64	1.90	1.00	1.45	1.81
12	0.63	2.45	1.69	2.86	1.25	1.71	1.14	1.60	1.96
	1.15	4.00	1.29	4.00	1.75	2.36	1.57	2.03	2.48
	1.17	5.34	1.33	4.29	1.50	2.36	1.03	1.35	1.65
	2.19	6.45	1.45	4.29	1.76	2.14	1.11	1.78	2.17
18	0.63	3.11	1.87	2.87	1.28	1.76	1.36	1.61	2.12
	1.15	4.78	1.48	4.12	1.65	2.35	1.74	2.03	2.68
	1.17	6.67	1.43	4.87	1.70	2.47	1.24	1.70	2.24
	2.19	9.12	1.86	5.50	2.00	2.47	1.40	2.00	2.64
24	0.63	3.78	2.13	3.00	1.35	1.79	1.48	1.69	2.03
	1.15	5.56	1.72	4.22	1.65	2.37	1.73	2.09	2.70
	1.17	8.01	1.57	5.33	1.92	2.68	1.65	2.20	2.85
	2.19	11.57	2.17	6.00	2.25	3.00	1.84	2.29	2.96

$$I_{fs} = \frac{\text{Bearing pressure of unreinforced layered foundations at } \frac{s_0}{D} (= q_s)}{\text{Bearing pressure of homogeneous clay beds at } \frac{s_0}{D} (= q_c)} \quad (6.1)$$

$$I_{fsgc} = \frac{\text{Bearing pressure of geocell – reinforced foundations at } \frac{s_0}{D} (= q_r)}{\text{Bearing pressure of homogeneous clay beds at } \frac{s_0}{D} (= q_c)} \quad (6.2)$$

$$I_{fgc} = \frac{\text{Bearing pressure of geocell – reinforced foundations at } \frac{s_0}{D} (= q_r)}{\text{Bearing pressure of unreinforced layered foundations at } \frac{s_0}{D} (= q_s)} \quad (6.3)$$

Variations of improvement factors, I_{fsgc} , with footing settlement, for different layered configurations on very soft clay subgrade ($c_u = 7$ kPa), are presented in Fig. 6.13. The figure also shows the improvement factors, I_{fs} , obtained for the unreinforced layered configurations. It can be observed that the improvement factors, I_{fsgc} and I_{fs} , are increased with increasing footing settlement. Variation of I_{fsgc} as 3.38–5.56 can be noted with footing settlement (s/D) in the range of 6–24%, for $c_u = 7$ kPa at $H = 1.15D$, while the corresponding variation in I_{fs} is 1.35–1.72. A

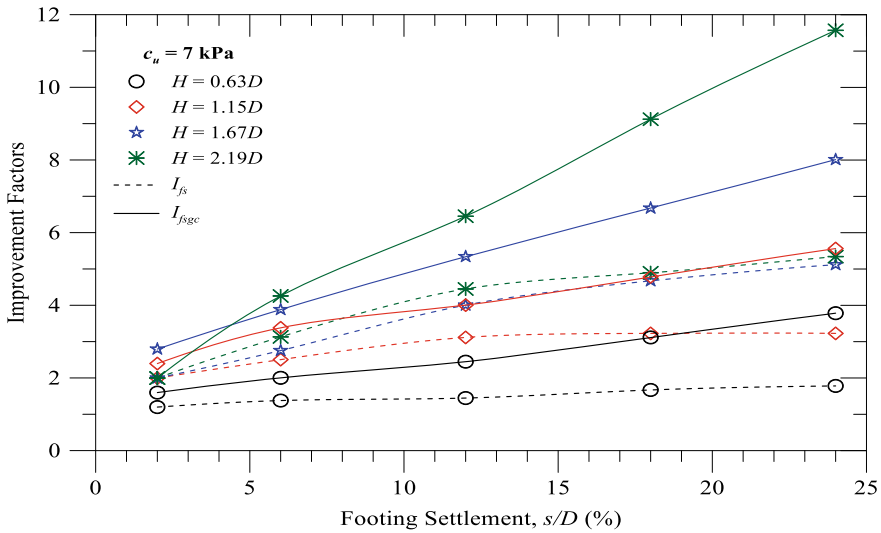


Fig. 6.13 Variation of I_{fs} and I_{fsgc} with s/D for $c_u = 7$ kPa

very high improvement factor of 11.6 is observed for $c_u = 7$ kPa, for the thickest geocell-matress of $h = 2.09D$ ($H = 2.19D$), at the largest settlement level tested ($s/D = 24\%$). This higher improvement in bearing pressure responses is contributed by the geocell-reinforcement.

Variations of I_{fgc} with footing settlement for different subgrades ($c_u = 7, 15, 30,$ and 60 kPa) are presented in Fig. 6.14, for two different layer thicknesses, such as $H = 0.63D$ and $1.15D$. It can be noticed that the variation of I_{fgc} , in Fig. 6.14, is not very consistent for all subgrades and for the layer thickness variations. However, in most of the cases, it was found increasing with settlement, showing more geocell contribution at higher strain.

Variations in improvement factors (I_{fs} and I_{fsgc}) for different subgrades (c_u) with varying layer thicknesses (H/D) are presented in Fig. 6.15 (at 12% of s/D). It is observed that the improvement factors are decreased with the increase in subgrade strength. At $H = 2.19D$, the improvement factor I_{fs} (dotted lines) is varied from 4.45 to 0.82 as the subgrade strength (c_u) increased from 7 to 60 kPa, while with geocell-reinforcement in similar condition, the I_{fsgc} variation is 6.45–1.78. However, at $H = 0.63D$, for both the foundation systems, the improvement factors (I_{fs} and I_{fsgc}) were greater for the subgrade having $c_u = 15$ kPa. The improvement factor, I_{fs} , was found as 2.29 compared to 1.45 (for $c_u = 7$ kPa), 1.5 (for $c_u = 30$ kPa), and 0.82 (for $c_u = 60$ kPa). Similarly, for 15 kPa, the I_{fsgc} was 2.86 compared to 2.45, 1.71, and 1.60, for $c_u = 7, 30,$ and 60 kPa, respectively. Due to the inclusion of geocell-reinforcements, the shearing of sand layer was arrested, and geocell-sand layer behaved like semi-rigid slab to increase the overall bearing capacity higher than the unreinforced layer configuration (even higher than the corresponding homogenous clay responses).

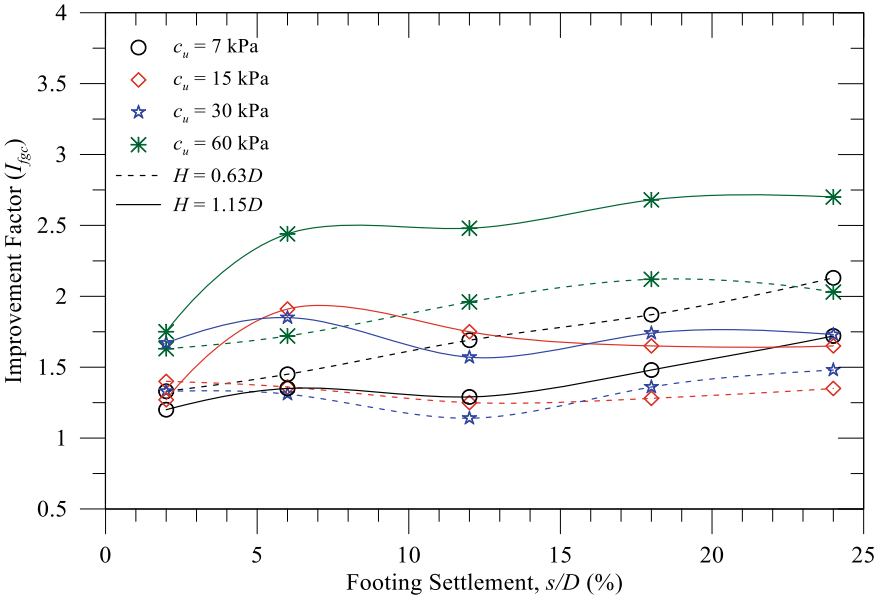


Fig. 6.14 Variation of I_{fgc} with s/D for different c_u at $H = 0.63$ and $1.15D$

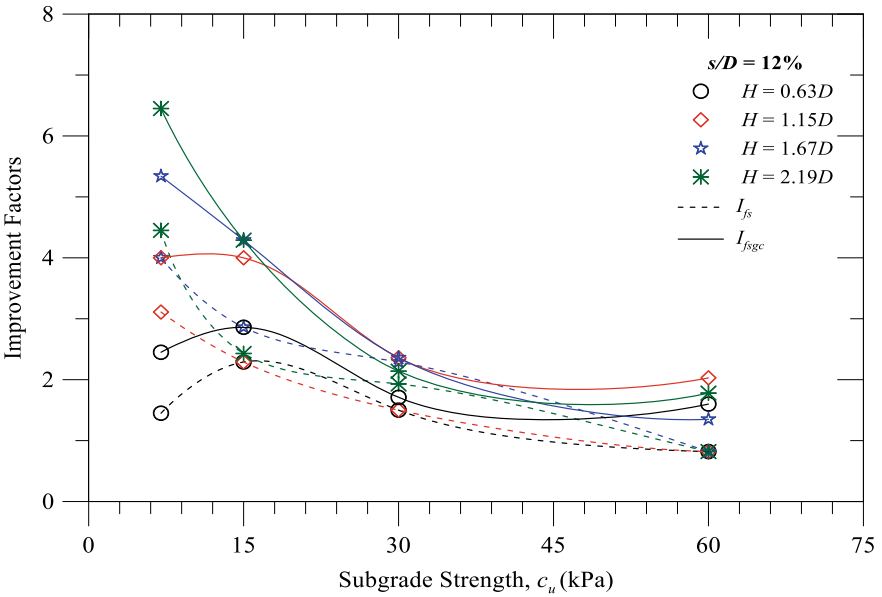


Fig. 6.15 Variation of I_{fs} and I_{fsgc} with c_u for different H/D at $s/D = 12\%$

6.4.3 Percentage Reduction in Settlement, PRS

The performance of geocell-reinforced foundations over clay beds of varying subgrade strength is also quantified with respect to reduction in footing settlements using a non-dimensional parameter described as “percentage reduction in settlement” (Sitharam et al. 2007). Referring Fig. 6.16, if s_o be the settlement of homogeneous beds and s_r be the settlement of geocell-reinforced foundation at a given pressure value q_o (corresponding to $s_o = 2, 6, 12, 18,$ and 24% of D), the percentage reduction in settlements (PRS) can be expressed as Eq. 6.4.

$$PRS = \frac{s_o - s_r}{s_o} \times 100\% \tag{6.4}$$

Figure 6.17 shows the variation in PRS with respect to subgrade clay strength (c_u) for different settlement levels ($s/D\%$). In general, the figure shows a trend of increase in PRS value with increase in s/D (%). The behavior indicates that the beneficial effect of geocell-reinforcements (confinement, interfacial resistance, and acting as semi-rigid slab) increases with increase in footing settlement. However, the trend for variation in PRS with respect to subgrade strength (c_u) is opposite as seen

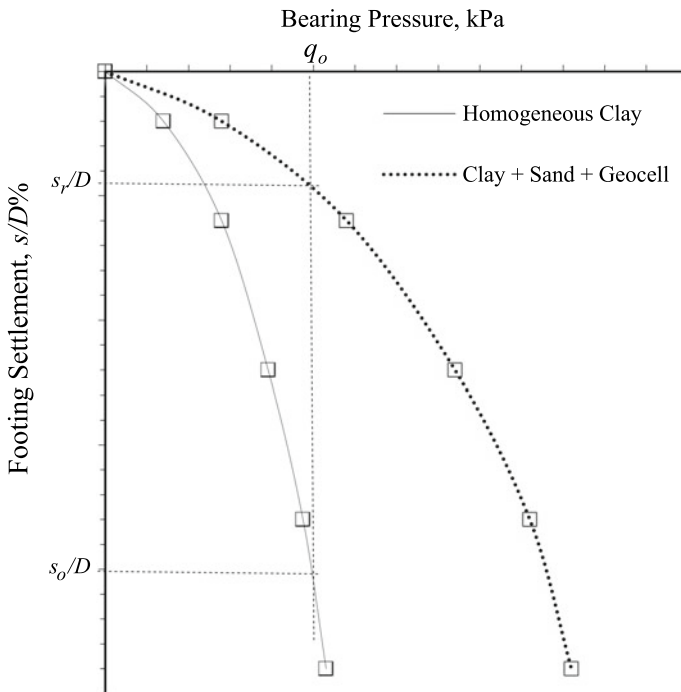


Fig. 6.16 Definition sketch for calculation of PRS

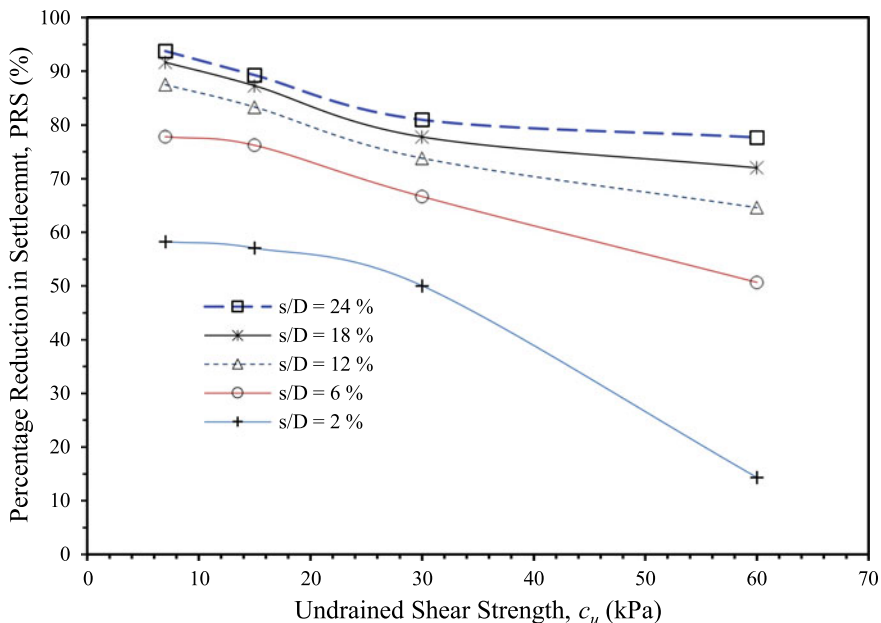


Fig. 6.17 Variation of PRS for different c_u at $H = 1.15D$

in case of s/D (%). The variation in PRS is decreased nonlinearly with increase in c_u . Though the settlements are significantly reduced even for higher subgrade strength soils, for lower subgrade strength soils, the reduction is more. For example, PRS values for c_u of 7 kPa ranged in between 60 and 95% for different settlement levels. The corresponding PRS values for c_u of 60 kPa are in the range of 15–80%.

6.5 Conclusion

This article reported observations from physical model tests carried out on model circular footing resting on foundation beds of different configurations having clay subgrades of varying strengths underneath. The responses obtained clearly indicated that the subgrade strength, irrespective of presence of reinforcement, largely influences the foundation behavior. The unreinforced sand layer favors softer clay subgrades ($c_u \leq 30$ kPa), while it affected negatively on stiff clay of 60 kPa. In the case of reinforced foundations, the introduction of geocell-reinforcement enhanced the reaction modulus (k_f) values significantly in comparison with corresponding values for unreinforced (homogeneous and layered) foundations. k_f values decrease with increase in settlement levels. For a given settlement level, k_f increased with increase in subgrade strength, indicating higher performance for clay subgrade with higher strength.

The reinforcements have positive impact on all clay subgrades; however, the degree of improvement, with reference to native subgrade soil capacity, reduced with increase in undrained strength of clay. The degree of improvement, both in terms of strength (I_{fsgc} or I_{fgc}) and settlement (PRS), with respect to homogeneous clay is considerably high in case of foundation with soft clay ($c_u = 7$ kPa), while it was reduced with increase in subgrade strength. Though the settlements are significantly reduced even for higher subgrade strength soils, for lower subgrade strength soils, the reduction is more. Thus, depending on the observations, it is concluded that the use of geocell and/or layers of compacted unreinforced soil (sand) must be in accordance to native subgrade strength. The degree of improvement expected to be achieved (both in terms of increase in bearing pressure and reduction in settlement) from reinforcement shall be evaluated according to the subgrade shear strength.

References

- Akinmusuru JO, Akinbolade JA (1981) Stability of loaded footings on reinforced soil. *J Geotech Eng Div, ASCE* 107(6):819–827
- Bathurst RJ, Rajagopal K (1993) Large scale triaxial compression testing of geocell reinforced granular soil. *Geotech Test J, GTJODJ* 16(3):296–303
- Binquet J, Lee KL (1975) Bearing capacity tests on reinforced earth slabs. *J Geotech Eng Div, ASCE* 101(12):1241–1255
- Biswas A, Krishna AM, Dash SK (2016) Behavior of geosynthetic reinforced soil foundation systems of different configurations over a stiff clay subgrade. *Int J Geomech ASCE*. [https://doi.org/10.1061/\(ASCE\)JGM.1943-5622.0000559](https://doi.org/10.1061/(ASCE)JGM.1943-5622.0000559)
- Biswas A (2016) Influence of subsoil strength on performance of geosynthetic-reinforced foundations. Ph.D. Thesis, IIT Guwahati, India
- Biswas A, Krishna AM (2017a) Behaviour of circular footing resting on layered foundation: sand overlying clay of varying strengths. *Int J Geotech Eng*. <https://doi.org/10.1080/19386362.2017.1314242>
- Biswas A, Krishna AM (2017b) Geocell-reinforced foundation systems: a critical review. *Int J Geosynthetics Gr Eng, Springer*. <https://doi.org/10.1007/s40891-017-0093-7>
- Biswas A, Dash SK, Krishna AM (2013) Parameters influencing the performance of geocell-reinforced foundation system: a brief review. In: *Proceedings of Indian geotechnical conference, IIT Delhi, vol 1, pp 365–368*
- Biswas A, Ansari MA, Dash SK, Krishna AM (2015) Behavior of geogrid reinforced foundation systems supported on clay subgrades of different strengths. *Int J Geosynthetics Gr Eng, Springer* 1(3):1–10
- Caroll RG, Curtis VC (1990) Geogrid connections. *Geotext Geomembr* 9(4–6):515–530
- Dash SK, Sireesh S, Sitharam TG (2003) Behaviour of geocell reinforced sand beds under circular footing. *Gr Improv* 7(3):111–115
- Fragaszy RJ, Lawton E (1984) Bearing capacity of reinforced sand subgrades. *J Geotech Eng Div, ASCE* 110(10):1500–1507
- Khing KH, Das BM, Puri VK, Yen SC, Cook EE (1994) Foundation on strong sand underlain by weak clay with geogrid at the interface. *Geotext Geomembr* 13(3):199–206
- Mandal JN, Sah HS (1992) Bearing capacity tests on geogrid-reinforced clay. *Geotext Geomembr* 11(3):327–333

- Pokharel SK, Han J, Leshchinsky D, Parsons RL, Halahmi I (2010) Investigation of factors influencing behaviour of single geocell-reinforced bases under static loading. *Geotext Geomembr* 28(6):570–578
- Rajagopal K, Krishnaswamy NR, Madhavi Latha G (1999) Behaviour of sand confined with single and multiple geocells. *Geotext Geomembr* 17(3):171–184
- Simac MR (1990) Connections for geogrid systems. *Geotext Geomembr* 9(4):537–546
- Sitharam GT, Sireesh S, Dash SK (2007) Performance of surface footing on geocell-reinforced soft clay beds. *Geotech Geol Eng* 25:509–524
- Sitharam TG, Sireesh S (2004) Model studies of embedded circular footing on geogrid reinforced sand beds. *Gr Improv* 8(2):69–75
- Webster SL, Watkins JE (1977) Investigation of construction techniques for tactical bridge approach roads across soft ground. Technical Report S-77-1, United State Army Corps of Engineers, Waterway Experiment Station, Mississippi, USA
- Yang X, Han J, Parsons RL, Leshchinsky D (2010) Three-dimensional numerical modelling of single geocell-reinforced sand. *Front Archit Civ Eng China* 4(2):233–240